Electronic Supplementary Material (ESI) for Journal of Materials Chemistry A.

Photostable organic solar cells based on non-fullerene acceptors with an aminated bathocuproine electron transport layer

Yong Ryun Kim[‡a,b], Sanseong Lee[‡c,e], Juae Kim[d], Juhui Oh[c,e], Ju-Hyeon Kim[c,e], Taeyoon Ki[c,e], Chang-Mok Oh[f], In-Wook Hwang[f], Hongsuk Suh[d*], Kwanghee Lee[a,c,e*], Heejoo Kim[a,g*]

[a)]*Research Institute for Solar and Sustainable Energies (RISE), Gwangju Institute of Science and Technology, Gwangju 61005, Republic of Korea*

[b)]*Department of Engineering, University of Cambridge, Cambridge, CB3 0FA, UK*

[c)]*School of Materials Science and Engineering, Gwangju Institute of Science and Technology, Gwangju 61005, Republic of Korea*

[d)]*Department of Chemistry and Chemistry Institute for Functional Materials, Pusan National University (PNU), Busan 46241, Republic of Korea*

[e)]*Heeger Center for Advanced Materials (HCAM), Gwangju Institute of Science and Technology, Gwangju 61005, Republic of Korea*

[f)]*Advanced Photonics Research Institute, Gwangju Institute of Science and Technology, Gwangju 61005, Republic of Korea.*

[g)]*Graduate School of Energy Convergence, Institute of Integrated Technology, Gwangju Institute of Science and Technology, Gwangju 61005, Republic of Korea*

‡ Y.R.K and S.L contributed equally to this work.

Address correspondence to *hssuh@pusan.ac.kr, klee@gist.ac.kr, heejook@gist.ac.kr*

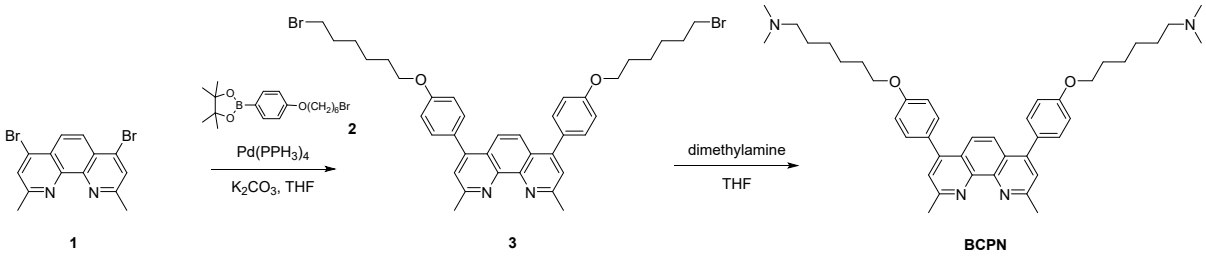

Scheme 1. Synthetic routes for the syntheses of the BCPN.

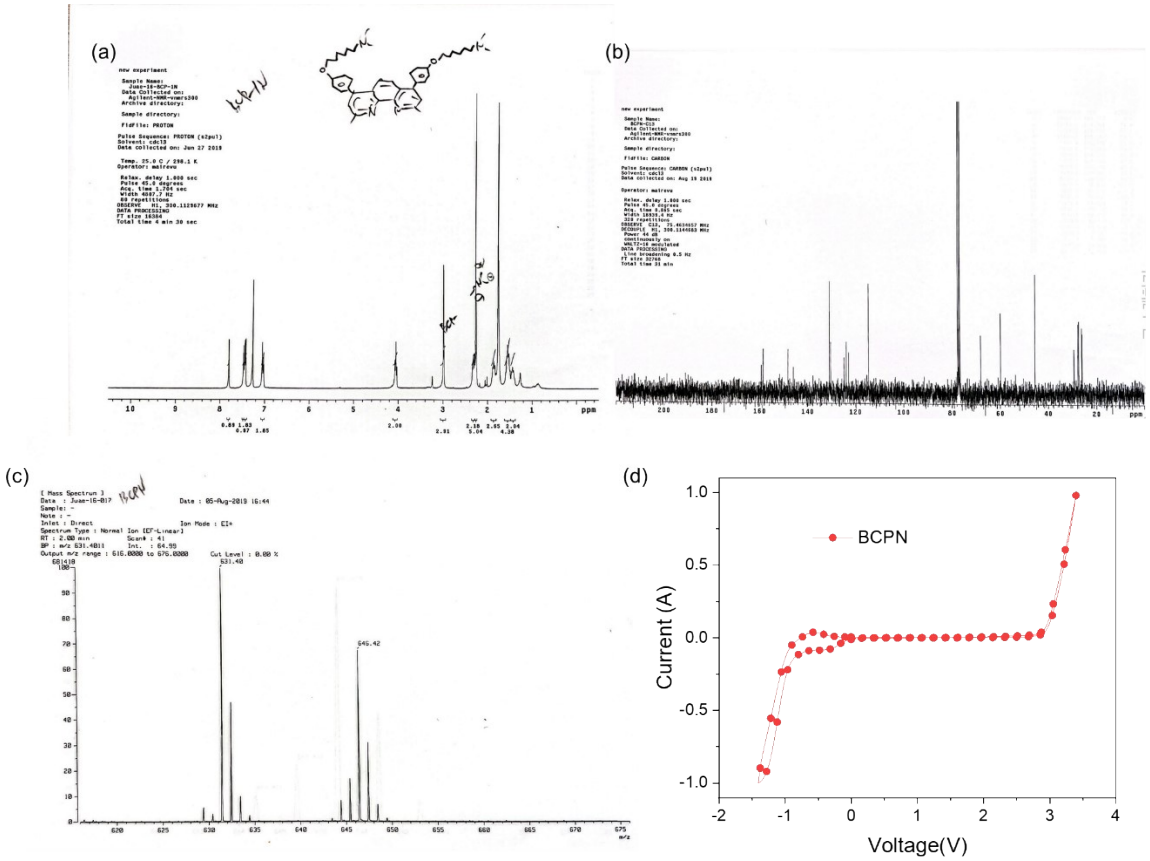

Fig. S1. (a) H^{1} NMR, (b) C^{13} NMR and (c) MS (MALDI-TOF) spectra of BCPN.

(d) Cyclic voltammetry curves of BCPN.

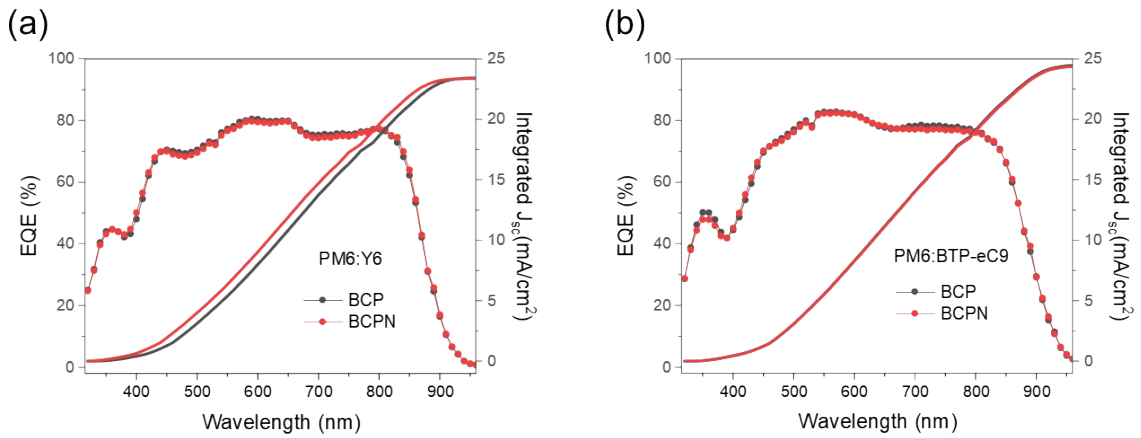

Fig. S2. The EQE spectra (dotted lines) and the integrated J_{sc}s (solid lines) for (a) PM6:Y6-based OSCs and (b) PM6:BTP-eC9-based OSCs built using BCP and BCPN ETLs.

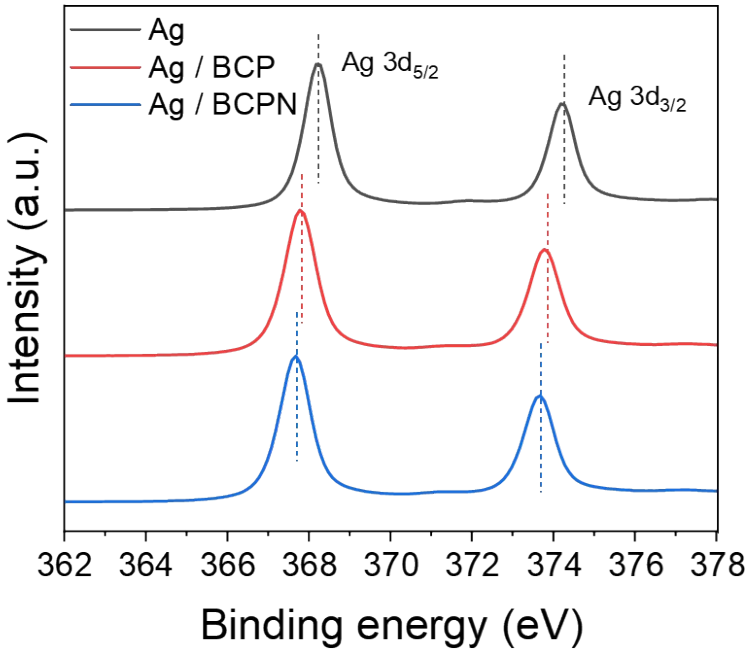

Fig. S3. The XPS spectra for Ag 3d core level peaks measured for the Ag bare film and Ag films coated with BCP and BCPN ETLs.

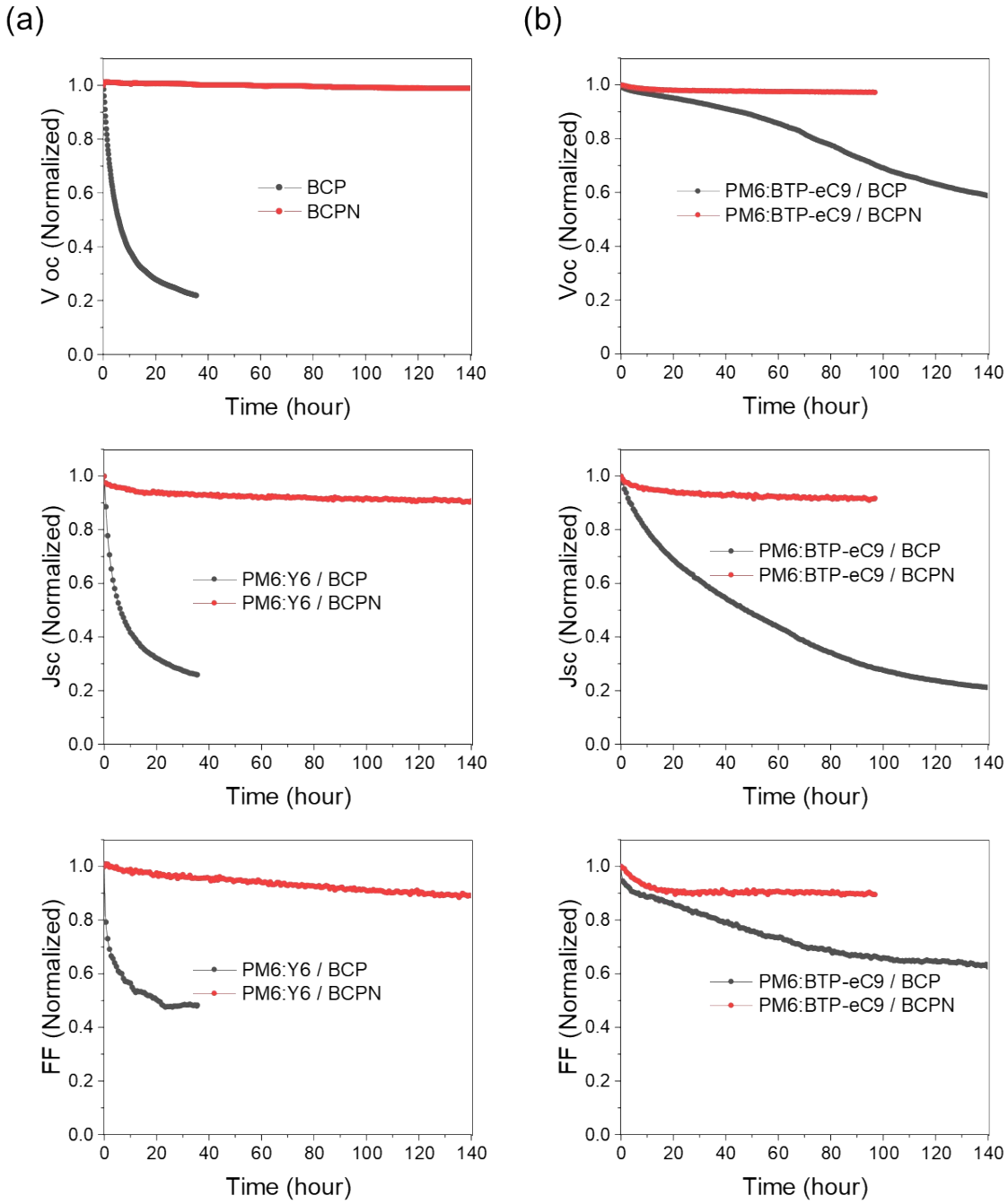

Fig. S4. Normalized V_{oc}, J_{sc} and FF values as a function of illumination time under 1 sun AM 1.5G spectrum illumination in N_2 gas for (a) PM6:Y6-based and (b) PM6:BTP-eC9-based devices built using BCP and BCPN ETLs.

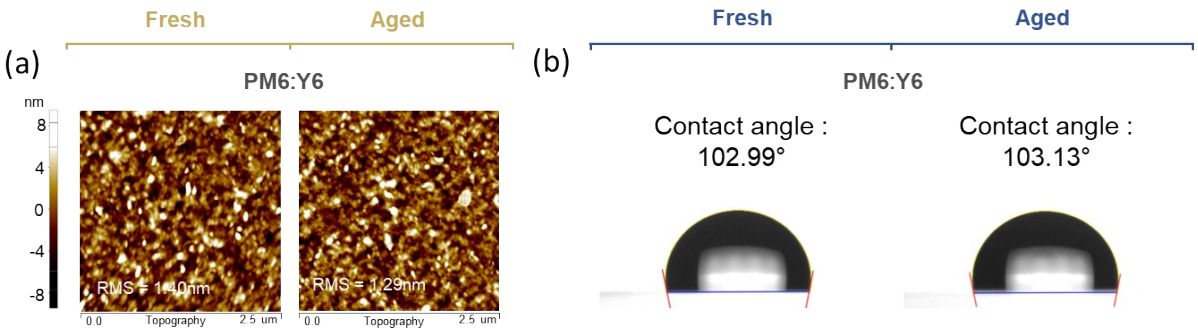

Fig. S5. (a) AFM height images and (b) water contact angles measured for PM6:Y6 layers before and after aging by illumination (AM 1.5G, 100 mW/cm^2).

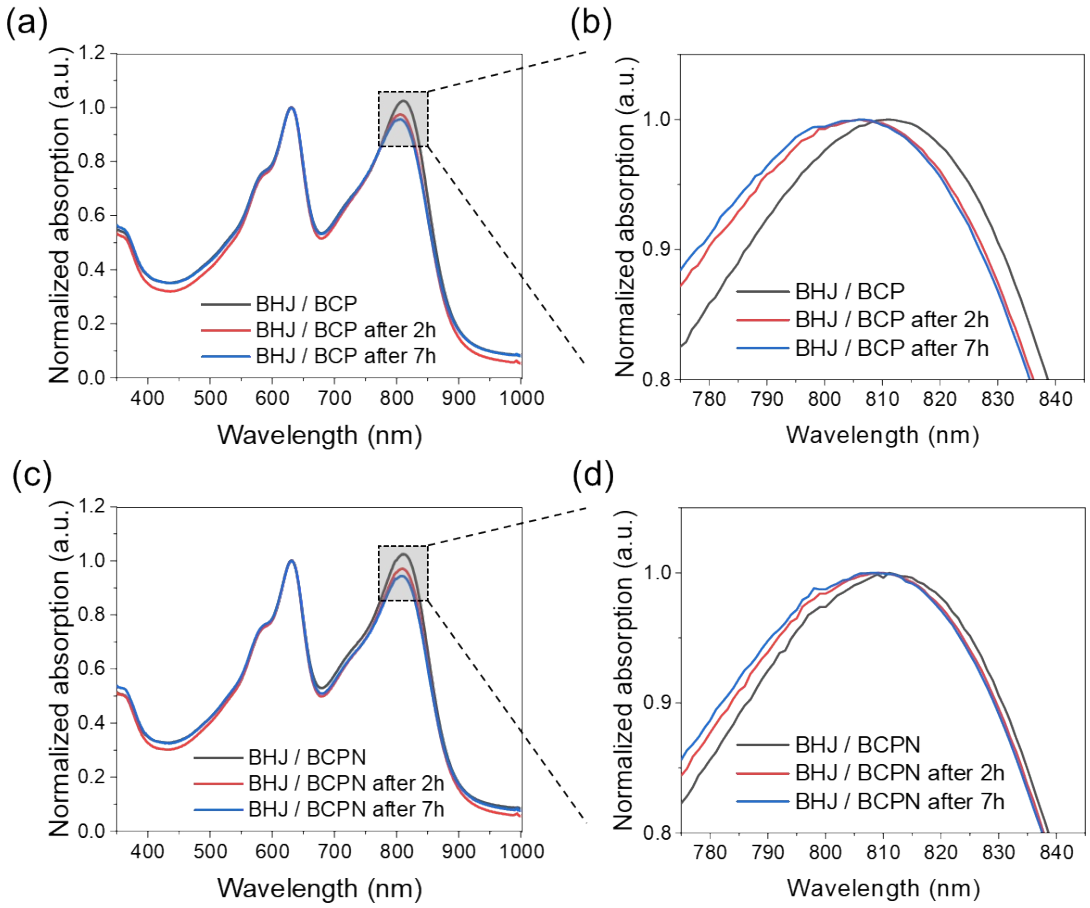

Fig. S6. Change in UV–Vis spectra (normalized by the 630 nm peak) measured for PM6:Y6 BHJ films coated with (a) BCP and (c) BCPN over illumination time in N_2-filled conditions. (b, d) UV–Vis spectra normalized by the maximum values obtained in the range indicated by the gray boxes shown on the corresponding full-range UV–Vis spectra.

Table S1. Photovoltaic parameters of NFA-based OSCs using BCP and BCPN ETLs with different active area.

BHJ layer	ETLs	Area (mm^2)	V_{oc} (V)	J_{sc} (mA/cm^2)	FF (%)	PCE (%)
PM6:Y6	BCP	4	0.846	24.31	70.5	14.50
		25	0.839	24.68	68.4	14.16
		36	0.815	24.86	63.5	12.87
		81	0.778	24.53	48.4	9.24
		100	0.837	24.62	47.5	9.79
	BCPN	4	0.835	26.25	71.0	15.57
		25	0.828	25.00	66.9	13.85
		36	0.821	24.78	62.6	12.74
		81	0.848	24.94	56.9	12.04
		100	0.849	24.55	53.4	11.13
PM6:BTP-eC9	BCP	4	0.807	27.75	74.6	16.72
		25	0.822	26.24	73.6	15.88
		36	0.813	25.14	70.3	14.38
		81	0.835	24.81	60.3	12.49
		100	0.837	25.06	57.9	12.14
	BCPN	4	0.828	26.25	77.3	16.81
		25	0.821	26.44	73.9	16.04
		36	0.820	25.92	70.6	14.99
		81	0.844	25.60	64.3	13.90
		100	0.842	25.96	58.8	12.86

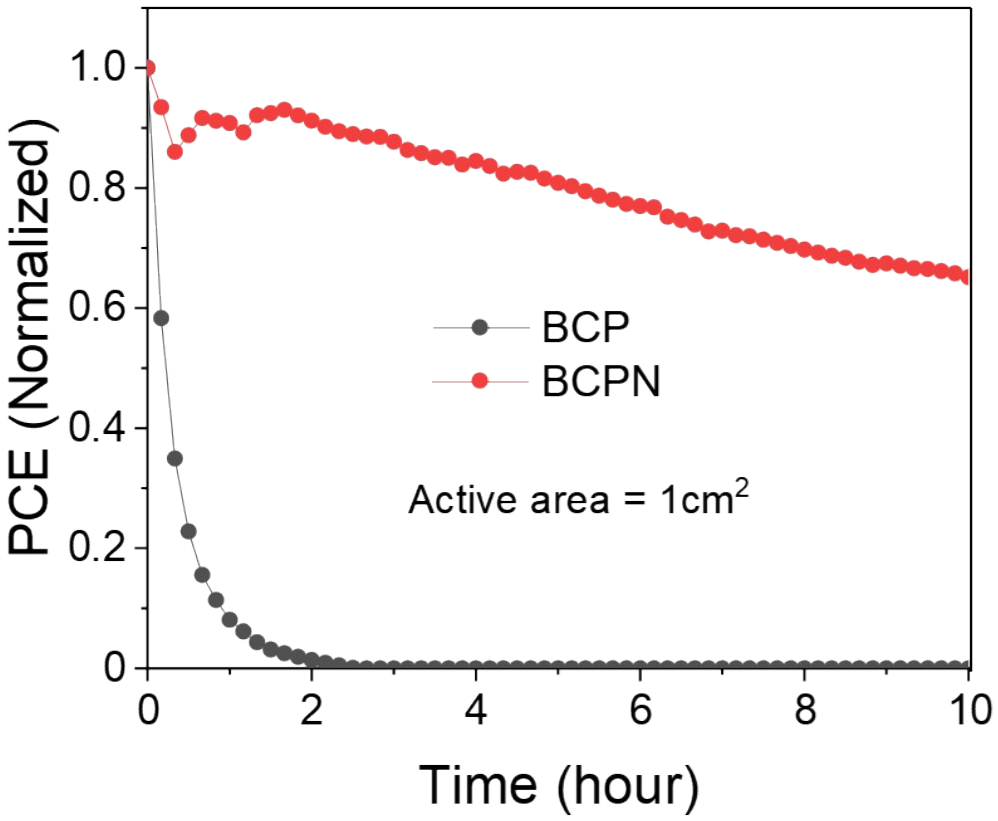

Fig. S7. Photostability measurement for PM6:Y6 solar cells with an area of 1 cm^2 under simulated solar light irradiation (AM 1.5 G, 100 mW/cm^2).

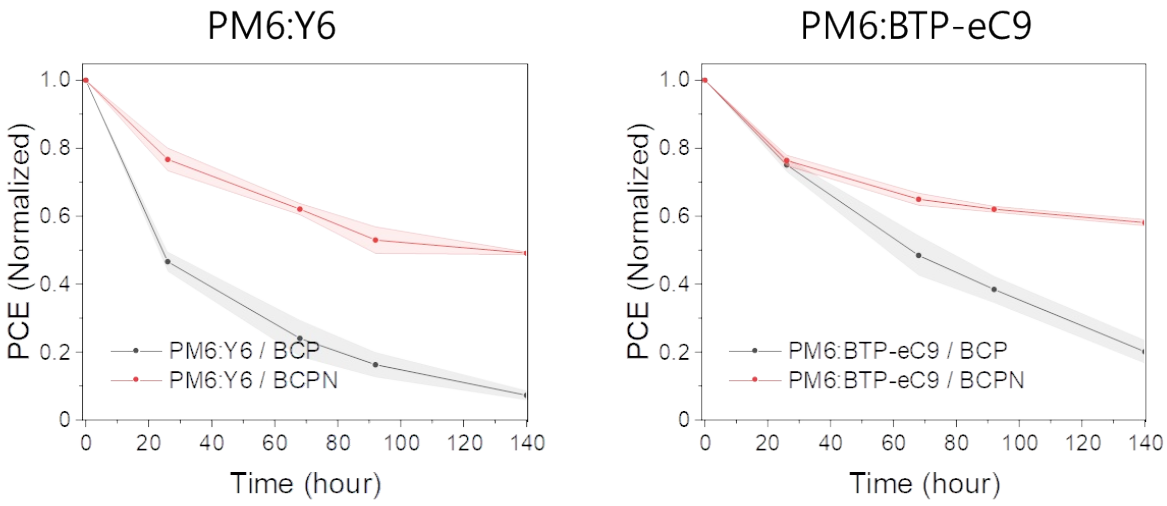

Fig. S8 - Air-stability performance of both PM6:Y6 and PM6:BTP-eC9 with different ETLs (BCP and BCPN) under ambient condition (20-40% relative humidity, T = 25°C)